

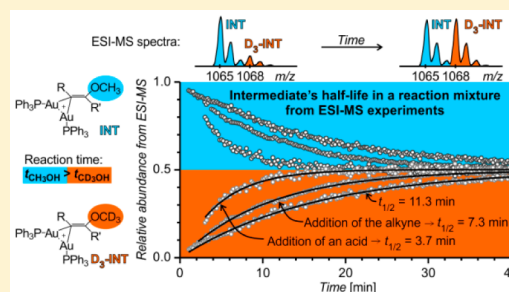
# Reaction Intermediates Kinetics in Solution Investigated by Electrospray Ionization Mass Spectrometry: Diaurated Complexes

Lucie Jašíková, Mariarosa Anania, Simona Hybelbauerová, and Jana Roithová\*

Department of Organic Chemistry, Faculty of Science, Charles University in Prague, Hlavova 2030/8, 12843 Prague 2, Czech Republic

**S** Supporting Information

**ABSTRACT:** A new method to investigate the reaction kinetics of intermediates in solution by electrospray ionization mass spectrometry is presented. The method, referred to as delayed reactant labeling, allows investigation of a reaction mixture containing isotopically labeled and unlabeled reactants with different reaction times. It is shown that we can extract rate constants for the degradation of reaction intermediates and investigate the effects of various reaction conditions on their half-life. This method directly addresses the problem of the relevance of detected gaseous ions toward the investigated reaction solution. It is demonstrated for geminally diaurated intermediates formed in the gold mediated addition of methanol to alkynes. Delayed reactant labeling allows us to directly link the kinetics of the diaurated intermediates with the overall reaction kinetics determined by NMR spectroscopy. It is shown that the kinetics of protodeauration of these intermediates mirrors the kinetics of the addition of methanol demonstrating they are directly involved in the catalytic cycle. Formation as well as decomposition of diaurated intermediates can be drastically slowed down by employing bulky ancillary ligands at the gold catalyst; the catalytic cycle then proceeds via monoaurated intermediates. The reaction is investigated for 1-phenylpropyne ( $\text{Ph-CC-CH}_3$ ) using  $[\text{AuCl}(\text{PPh}_3)]/\text{AgSbF}_6$  and  $[\text{AuCl}(\text{IPr})]/\text{AgSbF}_6$  as model catalysts. Delayed reactant labeling is achieved by using a combination of  $\text{CH}_3\text{OH}$  and  $\text{CD}_3\text{OH}$  or  $\text{Ph-CC-CH}_3$  and  $\text{Ph-CC-CD}_3$ .



## INTRODUCTION

Mass spectrometry (MS) is an important tool for the investigation of reaction mechanisms.<sup>1–5</sup> The introduction of electrospray ionization (ESI) allowed direct probing of reaction mixtures and ESI-MS was established as a method for “fishing out” reaction intermediates.<sup>6,7</sup> A big advantage of using ESI-MS is its sensitivity. Reactive intermediates that are often present at very low concentrations can be detected, isolated in the gas phase and can have their reactivity probed.<sup>8–10</sup> The structure of the intermediates can be interrogated in collisional experiments or with ion spectroscopy approaches.<sup>11,12</sup>

The limitations of ESI-MS always have to be considered. For example, the relative intensities of the peaks in a mass spectrum do not need to correlate with the concentrations in the sprayed solution.<sup>13</sup> Indeed the same reaction mixture can provide completely different ESI-MS spectra if the ionization conditions are changed.<sup>14–16</sup> Given common instabilities in the ionization conditions and an unknown response to the concentration of the ionized species, the use of ESI-MS to monitor reaction kinetics is often associated with a large error or even not applicable. This obstacle can be somewhat circumvented by incorporating a permanently charged group into a reactant and assuming that the transfer of all ions containing this charged group to the gas phase will be similarly efficient.<sup>17,18</sup> This approach can be rather synthetically demanding and cannot be

generally used; for example if the reaction intermediates are naturally cationic or anionic.

Another complicating feature of ESI-MS is possible artifacts from the electrospray process. Electrospray ionization is associated with increasing the concentration of the sprayed solution by several orders of magnitude, so exotic species can be formed although they did not exist in the original solution. The concurrent method for the investigation of reaction mechanisms and reaction intermediates is nuclear magnetic resonance (NMR) spectroscopy. This method is largely complementary to ESI-MS. Direct examination of a reaction mixture assures the sole detection of relevant species and the most commonly applied <sup>1</sup>H NMR has a linear response to the concentration of the given species in solution.<sup>19</sup> Nevertheless, all species are investigated at once, so reactive intermediates that are present in negligible amounts are usually not detected.

Here, we present a new method for the investigation of reaction intermediates using ESI-MS. This method is based on monitoring a reaction mixture containing one of the reactants as a mixture of isotopically labeled and unlabeled molecules. Either the labeled or unlabeled molecules are added to the reaction mixture with a time delay. As detailed below, this trick provides a direct link to the condensed phase and helps

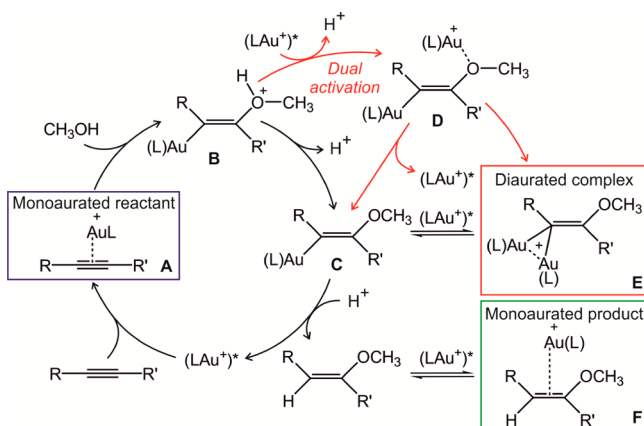
Received: August 18, 2015

Published: October 2, 2015

eliminate artifacts from the electrospray ionization process. This opens the possibility of investigating the kinetics of all possible complexes containing this particular reactant during a given reaction.

The new method will be applied to monitor the kinetics of diaurated intermediates<sup>20</sup> in the gold(I) mediated addition of methanol to alkynes (Scheme 1).<sup>21–26</sup> We have chosen 1-

**Scheme 1. Combination of Suggested Reaction Mechanisms for Gold(I) Catalyzed Addition of Methanol to an Alkyne**<sup>13,26–33a</sup>



<sup>a</sup>Complexes in the frames can be detected by ESI-MS.<sup>13</sup> The symbol  $(\text{LAu}^+)^*$  is used for an active form of the catalyst.

phenylpropyne as a model alkyne and  $[\text{AuCl}(\text{PPh}_3)]$  and  $[\text{AuCl}(\text{IPr})]$  (IPr = 1,3-bis(2,6-diisopropylphenyl)imidazol-2-ylidene) as representative catalysts. It has been shown that with a gold catalyst bearing a small ligand such as trimethylphosphine or triphenylphosphine the reaction proceeds via the formation of geminally diaurated complexes, which are subsequently protodeaurated to form the product of the reaction.<sup>13,27</sup> Using gold catalysts with bulky ligands, such as the *N*-heterocyclic carbene ligand IPr, leads to a suppression of the formation of diaurated intermediates and renders the reaction faster. If the geminally diaurated complexes are formed with the bulky ligands, then it was shown that they do not undergo subsequent protodeauration and remain as byproducts of the reaction.<sup>27</sup>

It was suggested that the geminally diaurated complexes are formed by the trapping of neutral monoaurated intermediates C by another  $[(\text{L})\text{Au}]^+$  cation (Scheme 1).<sup>28–33</sup> The trapping reaction  $\text{C} \rightarrow \text{E}$  has been suggested to be reversible for catalysts with small phosphine ligands, or irreversible for catalysts bearing bulky ligands.<sup>27</sup> We have previously suggested that the diaurated complexes are not formed by an off-cycle trapping reaction, but instead are the result of the primary formation of the geminally diaurated intermediate E.<sup>13</sup> Originally, we proposed  $[(\text{L})\text{Au}(\text{OCH}_3)]$  addition to the gold-activated alkyne, but the exchange of the hydrogen atom of the methanol molecule can also proceed at intermediate B as depicted.

The presented “delayed reactant labeling” method in ESI-MS enables us to study various effects such as the acidity of the reaction mixture or silver cation concentration on the half-life of the diaurated intermediates and relate it to the reaction kinetics obtained by NMR spectroscopy.

## EXPERIMENTAL AND COMPUTATIONAL DETAILS

Reaction mixtures were prepared by mixing a filtered solution of  $\text{AgSbF}_6$  and  $[\text{AuCl}(\text{PPh}_3)]$  (or  $[\text{AuCl}(\text{IPr})]$ , where IPr = 1,3-bis(2,6-diisopropylphenyl)imidazol-2-ylidene) in methanol (either  $\text{CH}_3\text{OH}$  or  $\text{CD}_3\text{OH}(\text{D})$ ) with 1-phenylpropyne (or  $\text{D}_3$ -1-phenylpropyne) so that a 0.24 M solution of ( $\text{D}_3$ -)1-phenylpropyne with 2.5 mol % of the  $[\text{AuCl}(\text{PPh}_3)]$  (or  $[\text{AuCl}(\text{IPr})]$ ) was formed.

The NMR experiments were recorded using a Bruker AVANCE III (600 MHz) and the  $\delta$  scale was referenced to the solvent residual peak at  $\delta = 3.31$  ppm. The solutions of a catalyst and reactants were mixed and immediately probed by the NMR instrument. The representative  $^1\text{H}$  NMR spectrum with peak assignments is shown in the Supporting Information, Figure S1.

Mass spectrometry experiments were performed on a TSQ 7000 mass spectrometer<sup>34,35</sup> with a quadrupole-octopole-quadrupole configuration. The ions were generated by electrospray ionization (ESI) at soft ionization conditions and the mass spectra were recorded by scanning the first quadrupole (Figures S3–S5 in the Supporting Information). For the mass spectrometry experiments, the reaction mixtures were diluted 10-times (hence 0.024 M solution of 1-phenylpropyne was used). The exact compositions of all investigated reaction mixtures are listed in the Supporting Information.

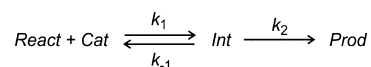
DFT calculations were performed using the B3LYP<sup>36</sup> density functional and D3 empirical correction<sup>37</sup> for the dispersion interactions as implemented in the Gaussian program package.<sup>38</sup> For the geometry optimization, the combination of the cc-pVTZ basis set for C, H, O, N and P and the LanL2DZ basis set for Au was used. Frequency calculations were performed in order to control the nature of the stationary points and obtain thermochemical corrections for enthalpies and free energies at 0 and 298 K. The solvent effect of methanol was approximated by single-point calculations using the polarized continuum model.<sup>39</sup> All optimized structures and their energies are listed in Table S10 in the Supporting Information. We have also studied the basis set effect at the gold atom. Results of single-point calculations with the LanL2TZ for Au and cc-pVTZ for the remaining atoms show that the effect is negligible (Table S8). The effect of the dispersion interactions was tested by B3LYP/cc-pVTZ(LanL2TZ for Au) single-point calculations without D3 empirical correction. The pathways leading via neutral monoaurated intermediates become endothermic (Table S9).

The energetics of protonation/deprotonation steps are strongly influenced by the method used for approximation of the proton enthalpy. We have tried to apply the published value for the proton enthalpy in methanol ( $-1054 \text{ kJ mol}^{-1}$ ),<sup>40</sup> but it renders all reactions where the proton is eliminated about  $50 \text{ kJ mol}^{-1}$  more endothermic (see Table S7 in the Supporting Information). Such a potential energy surface would basically exclude the reaction pathways leading via neutral monoaurated intermediates, therefore we did not apply it here. Instead, proton was considered in the form of proton-bound dimer of methanol. Under this assumption, formation of a neutral monoaurated intermediate becomes exothermic.

## KINETIC MODEL

Our kinetic model is derived from the very simple model shown in Scheme 2. We assume a first-order reaction between a

**Scheme 2**



catalyst (Cat) and a reactant (React) yielding an intermediate (Int). The intermediate then transforms to a product (Prod). This model can be straightforwardly improved by taking into account particularities of a given studied system, but to demonstrate our method it will be used in this simplest version. Such kinetic schemes allow us to express the time evolution of

the intermediate concentrations as well as the concentrations of the reactants and products. It can be easily applied for NMR kinetic experiments, in which we follow concentration changes of reactants, products, and sometimes also intermediates.

The ESI-MS method suffers from a nonlinear response to the concentration of species in the solution as outlined in the Introduction. The concentration changes have to be therefore approached indirectly. We have designed a method with delayed labeling of the reaction mixture by an isotopically labeled reactant while the mixture also contains the corresponding unlabeled reactant. The corresponding mass spectrum shows pairs of signals of ions containing the reactants. We assume that the ionization efficiencies are not influenced by the isotopic labeling. The key trick is the time delay in the labeling. The mutual time evolution of the unlabeled and labeled signal intensities reflects the kinetics of formation and depletion of the given intermediate. The overall intensities of the signals are therefore not important, because we evaluate the signals only relative to each other. We demonstrate the utility of this approach for the investigation of intermediates whose formation and depletion can be described by a steady-state approximation (eq 1).

$$k_1[\text{Cat}][\text{React}] = (k_{-1} + k_2)[\text{Int}]_{\text{eq}} \quad (1)$$

The reaction mixture is first prepared with unlabeled reactants (React) and allowed to react for time  $t_d$ . During this time a certain concentration of the intermediate [Int] is achieved. After  $t_d$  elapses, the labeled reactant (React<sup>label</sup>) is added to the reaction mixture, which takes the reaction mixture away from the steady state conditions. At this time ( $t_0$ ), we start to monitor the reaction mixture by ESI-MS and record the abundances of the labeled and unlabeled ions (Figure 1). The

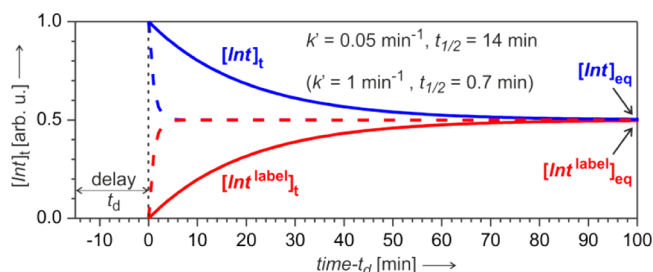


**Figure 1.** Ideal time evolution of the ESI-MS signals of unlabeled and labeled intermediates with different half-lives ( $t_{1/2}$ ). The labeled intermediate (Int<sup>label</sup>) was added to the reaction mixture with a time delay  $t_d$ . The solid lines show the signals time evolution for intermediates with  $t_{1/2} = 14$  min and the dashed lines for those with  $t_{1/2} = 0.7$  min.

time evolution of the corresponding signals reflects the reestablishment of the steady state conditions in the solution (eq 2).

$$\begin{aligned} \frac{d[\text{Int}]}{dt} &= (k_{-1} + k_2)[\text{Int}]_{\text{eq}} - (k_{-1} + k_2)[\text{Int}] \\ &= k'([\text{Int}]_{\text{eq}} - [\text{Int}]), \text{ where } k' \\ &= k_{-1} + k_2 \end{aligned} \quad (2)$$

At the time of mixing  $t_0$  the concentration of the labeled intermediate is zero ( $[\text{Int}^{\text{label}}]_0 = 0$ ). If we normalize  $[\text{Int}] + [\text{Int}^{\text{label}}] = 1$ , then the time evolution of the Int and Int<sup>label</sup> signals (blue and red lines in Figure 1) can be described as

$$[\text{Int}]_t = e^{-k't} + [\text{Int}]_{\text{eq}}(1 - e^{-k't}) \quad (3a)$$

and

$$[\text{Int}^{\text{label}}]_t = [\text{Int}^{\text{label}}]_{\text{eq}}(1 - e^{-k't}) \quad (3b)$$

For the given ideal experiment is  $[\text{Int}]_{\text{eq}} = [\text{Int}^{\text{label}}]_{\text{eq}} = 0.5$ . In the real experiments, we fit these values and obtain an accurate ratio of the intermediates in the given reaction mixture at the given reaction time. The half-life of the intermediate is determined as  $\ln 2/k'$ . Note that only the decomposition of the intermediates is studied ( $k'$ ). The rate of their formation ( $k_1$ ) does not influence the curve shapes, if we assume that both, labeled and unlabeled intermediates are formed with the same rate constant  $k_1$ .

While this model allows us to follow the kinetics of intermediates in reaction mixtures, it cannot be applied for every reaction. For example, if the half-life of the intermediate is very short, the current technique is not fast enough to monitor it. The dashed lines in Figure 1 show the steady state conditions establishment for an intermediate with  $k' = 1 \text{ min}^{-1}$  (half-life  $\sim 0.7$  min). Clearly, taking into account a time required for the mixing of the reaction mixtures and setting up the ESI-MS experiment, we cannot determine the relevant rate constant. For such a situation, we only observe the relative concentrations of the unlabeled and labeled intermediates ( $[\text{Int}]_{\text{eq}}$  and  $[\text{Int}^{\text{label}}]_{\text{eq}}$ ).

Before addressing the details of this method, we should point out that the labeling should be remote so that it does not affect the rate of the studied reaction. Hence, we assume that the labeled as well as the unlabeled reactant react with the same rate constants. We also note that it does not matter, whether the reaction time of the unlabeled or the labeled reactant is longer. For the sake of simplicity, we usually start with unlabeled reactant, but we have also performed the experiments in the reversed order and obtained the same results.

## RESULTS

**NMR Experiments.** To discuss the role of the diaurated intermediates in the reaction, we have first determined the kinetics of the formation of the products in the gold(I)-catalyzed methanol addition to 1-phenylpropyne by NMR (Scheme 1 and Figure 2). The methanol addition can take place either to the C(1) carbon atom or the C(2) carbon atom of 1-phenylpropyne and proceeds twice to form a methylvinylether in the first step and a ketal in the second step (Figure 2). The rate of the individual steps depends critically on the catalyst used. From comparison of  $[\text{AuCl}(\text{PPh}_3)]/\text{AgSbF}_6$  and  $[\text{AuCl}(\text{IPr})]/\text{AgSbF}_6$  it is clear that the latter catalyst provides a much faster conversion with more than 99% reactant consumption after 35 min. In a comparable time the conversion in the  $[\text{AuCl}(\text{PPh}_3)]$  catalyzed reaction only reaches about 10%.

Kinetic modeling of the NMR monitored reactions reveals a fundamental difference between the catalysts. Using the catalyst with the phosphine ligand renders the first reaction step about 2 orders of magnitude slower than that with the catalyst with the *N*-heterocyclic carbene ligand (Table 1). On the other hand, the second methanol addition is several times faster using the phosphine ligand. Clearly, the first methanol addition is the rate-determining step and the obvious explanation for the retarded rate of the reaction catalyzed by  $[\text{AuCl}(\text{PPh}_3)]$  is the formation of the diaurated intermediates. In the second

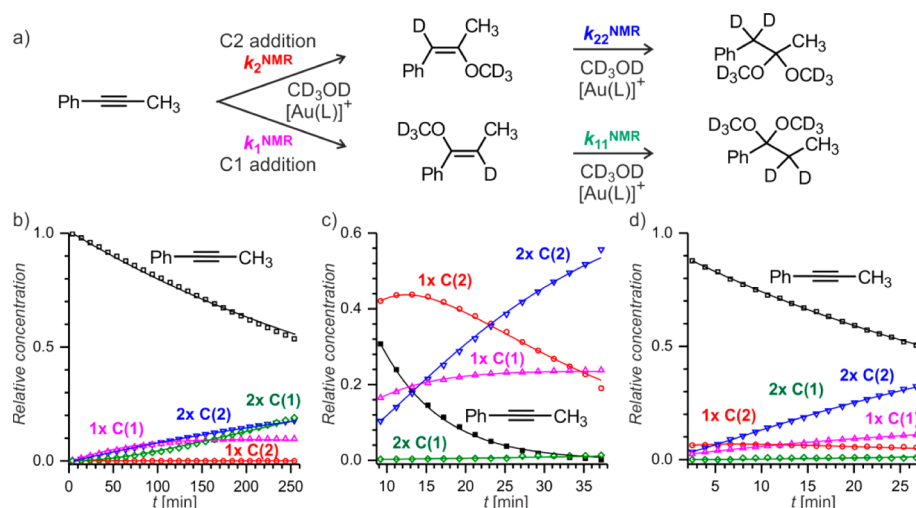


**Figure 2.** (a) Reaction scheme for the kinetic model of gold-mediated methanol addition to 1-phenylpropyne. (b–d) Relative ratios of 1-phenylpropyne and the methanol addition products in dependence of the reaction time catalyzed by (a) 2.5 mol % [AuCl(PPh<sub>3</sub>)]/3 mol % AgSbF<sub>6</sub>, (b) 2.5 mol % [AuCl(IPr)]/3 mol % AgSbF<sub>6</sub>, and (c) 1.25 mol % [AuCl(PPh<sub>3</sub>)]/1.25 mol % [AuCl(IPr)]/3 mol % AgSbF<sub>6</sub> as monitored by NMR spectroscopy. The yield of 1-phenyl-1-methoxypropene and 1-phenyl-2-methoxypropene is shown in pink and red. Products of the addition of two molecules of methanol (sum of the corresponding ketals and ketones formed upon hydrolysis with residual moisture) are shown in green for the C(1) addition and in blue for the C(2) addition. The solid lines correspond to fits obtained by the *Octave* program assuming the reaction scheme in (a). The corresponding rate constants are listed in Table 1.

**Table 1.** Rate Constants for the Gold(I) Mediated Methanol Addition to 1-Phenylpropyne Determined by the Kinetic Modelling of the Reaction Yields Monitored by NMR

catalyst	$k_1^{\text{NMR}}$	$k_2^{\text{NMR}}$	$k_{11}^{\text{NMR}}$	$k_{22}^{\text{NMR}}$
	dm <sup>3</sup> mol <sup>-1</sup> min <sup>-1</sup>			
2.5 mol % [AuCl(PPh <sub>3</sub> )]/ 3 mol % AgSbF <sub>6</sub>	0.19 ± 0.03	0.12 ± 0.02	1.3 ± 0.3	51 ± 14 <sup>a</sup>
2.5 mol % [AuCl(PPh <sub>3</sub> )]/ 3 mol % AgSbF <sub>6</sub> /TsOH	0.26 ± 0.01	0.18 ± 0.01	3.4 ± 0.8	56 ± 40 <sup>a</sup>
2.5 mol % [AuCl(IPr)]/ 3 mol % AgSbF <sub>6</sub>	5.6 ± 0.3	16.9 ± 0.9	0.3 ± 0.1	7.2 ± 0.7
2.5 mol % [AuCl(IPr)]/ 3 mol % AgSbF <sub>6</sub> /TsOH	7.2 ± 0.9	30 ± 6	1.4 ± 0.3	120 ± 4
1.25 mol % [AuCl(PPh <sub>3</sub> )]/1.25 mol % [AuCl(IPr)]/ 3 mol % AgSbF <sub>6</sub>	1.0 ± 0.1	2.5 ± 0.3	3 ± 2	27 ± 5
1.25 mol % [AuCl(PPh <sub>3</sub> )]/1.25 mol % [AuCl(IPr)]/ 3 mol % AgSbF <sub>6</sub> /TsOH	1.1 ± 0.2	3.8 ± 0.2	2 ± 1	81 ± 15
2.5 mol % [AuCl(PMe <sub>3</sub> )]/ 3 mol % AgSbF <sub>6</sub> <sup>b</sup>	0.15 <sup>b</sup>	0.42 <sup>b</sup>	0.85 <sup>b</sup>	(42) <sup>a,b</sup>

<sup>a</sup>The large experimental error is given by a negligible abundance of the product of single methanol addition to the C(2) carbon atom. The second step is 2 orders of magnitude faster, but the exact number can be determined only with large error bars. <sup>b</sup>Values are derived from previously published kinetics for the very same reaction performed under the same condition with the [AuCl(PMe<sub>3</sub>)] catalyst.<sup>13</sup>

methanol addition, the diastereotyped intermediates cannot be formed and correspondingly, the second methanol addition is even faster with [AuCl(PPh<sub>3</sub>)] catalysis than with [AuCl(IPr)] catalysis as could be anticipated based on the larger steric hindrance of the IPr ligand in the final protodeauration step.

The regioselectivity of the reaction can be controlled electronically or sterically. For the bulky catalyst [AuCl(IPr)], the addition preferentially proceeds at the C(2) carbon atom. This regioselectivity is thermodynamically favored (see also results of DFT calculations).<sup>13</sup> Using the [AuCl(PPh<sub>3</sub>)] catalysts, the C(1) addition is slightly preferred. We have also tested the effect of acid addition. The addition of 4 mol % of *p*-toluenesulfonic acid (TsOH) to the reaction mixture of both catalytic systems led to acceleration of the reaction (Table 1). The first step of the reaction is accelerated 1.3–1.8 times. The acceleration is more pronounced for C2 addition and it is rather similar for both catalysts. The effect in the second step exceeds that in the first step and it is more pronounced for the [AuCl(IPr)] catalyst. Once again, the effect for C(2) addition is larger.

We have also performed an experiment, in which we have used the same amount of gold(I) catalyst, but one-half was

bearing the triphenylphosphine ligand and the other half bears the NHC ligand. This combination led to a significant drop of the rate of the first reaction step in comparison to the reaction catalyzed by [AuCl(IPr)] only (to about one-seventh) and a slight drop of the second step rate. The effect of the acid addition was less pronounced than for the reactions with the individual catalysts.

If we compare the present results to the previously published results for the very same reaction performed under the same conditions, but using the [AuCl(PMe<sub>3</sub>)] catalyst, we can see that similar to the reaction catalyzed by [AuCl(PPh<sub>3</sub>)], the second reaction step is faster than the first one. The regioselectivity of the reaction favors formation of the C(2) products.

**ESI-MS Experiments.** The same reaction mixtures investigated by NMR were also probed by ESI-MS. The spectra (Figures S3–S5 in the Supporting Information) contain signals corresponding to the gold complexes bearing the auxiliary ligand L and either methanol ([L(Au(MeOH))]<sup>+</sup>), or 1-phenylpropyne ([L(Au(PhCCMe))]<sup>+</sup>), or the primary reaction product ([L(Au(PhCCMe,MeOH))]<sup>+</sup>), observed only for L = IPr). In addition, signals of the diastereotyped complexes

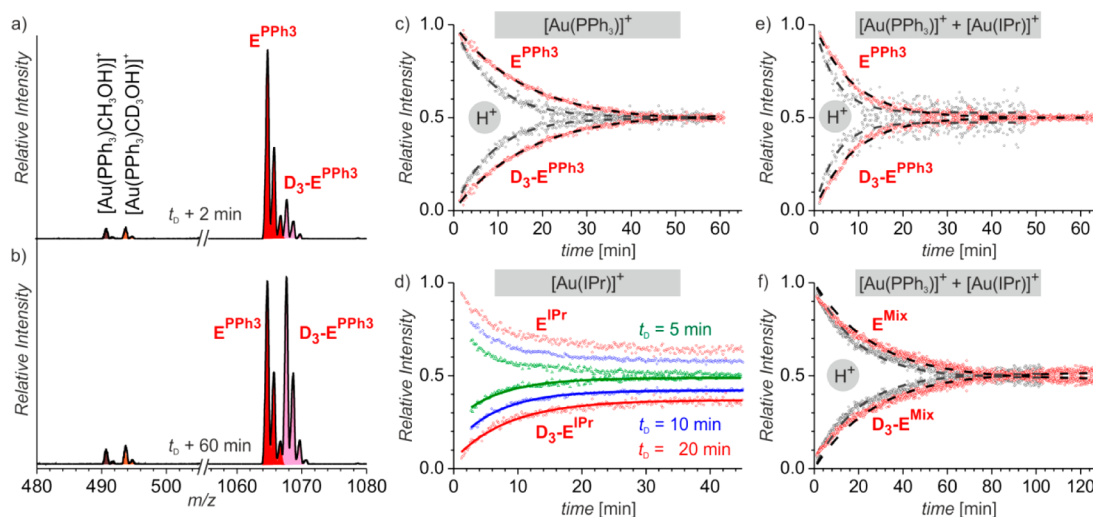


**Figure 3.** Delayed reactant labeling method. (a) ESI-MS spectrum recorded 2 min after the  $\text{CD}_3\text{OH}$  addition to the reaction mixture of 1-phenylpropyne with 2.5 mol %  $[\text{AuCl}(\text{PPh}_3)]$  and 3 mol %  $\text{AgSbF}_6$  in  $\text{CH}_3\text{OH}$ ; time-delay was 5 min. (b) The same as (a), but the ESI-MS spectrum was recorded 60 min after the labeling of the reaction mixture. (c) Mutual time evolution of the  $\text{E}^{\text{PPh}_3}$  and  $\text{D}_3\text{-E}^{\text{PPh}_3}$  signals in the experiment described in (a) (red symbols). The gray symbols show the effect of the  $\text{TsOH}$  addition to the reaction mixture. The dashed lines correspond to the data fits according to eq 3a and 3b. (d) Mutual signal evolution of  $\text{E}^{\text{IPr}}$  and  $\text{D}_3\text{-E}^{\text{IPr}}$  after the  $\text{CD}_3\text{OH}$  delayed labeling of the reaction mixture of 1-phenylpropyne with 2.5 mol %  $[\text{AuCl}(\text{IPr})]$  and 3 mol %  $\text{AgSbF}_6$  in  $\text{CH}_3\text{OH}$  with variable time delays (color coded). The lines represent fits according to eq 4. Mutual time evolutions of the (e)  $\text{E}^{\text{PPh}_3}$  and  $\text{D}_3\text{-E}^{\text{PPh}_3}$  and (f)  $\text{E}^{\text{Mix}}$  and  $\text{D}_3\text{-E}^{\text{Mix}}$  signals in the experiment with 1.25 mol %  $[\text{AuCl}(\text{PPh}_3)]$ , 1.25 mol %  $[\text{AuCl}(\text{IPr})]$ , and 3 mol %  $\text{AgSbF}_6$  in  $\text{CH}_3\text{OH}$  (red symbols). Delayed labeling with  $\text{CD}_3\text{OH}$  and  $t_d = 5$  min. The gray symbols are obtained from the same experiment but with the  $\text{TsOH}$  addition. The dashed lines correspond to the data fits according to eq 3a and 3b.

$[(\text{L})_2\text{Au}_2(\text{PhCCMe,OMe})]^+$  are observed. We have applied delayed reactant labeling to the reaction mixtures (see the Experimental Details) and monitored the kinetics of the degradation of the diaurated intermediates. Figure 3a,b show the relevant parts of the ESI-MS spectra of the reaction mixture with the  $[\text{Au}(\text{PPh}_3)]^+$  catalyst prepared in  $\text{CH}_3\text{OH}$  and labeled with a delay of 5 min with  $\text{CD}_3\text{OH}$ . It can be clearly seen that shortly after the labeling of the reaction mixture, the concentration of the unlabeled diaurated intermediate  $[(\text{PPh}_3)_2\text{Au}_2(\text{PhCCMe, OCH}_3)]^+$  ( $\text{E}^{\text{PPh}_3}$ ) was much higher than that of the labeled intermediate  $\text{D}_3\text{-E}^{\text{PPh}_3}$  (Figure 3a). After about 60 min, the concentration of both, the labeled and unlabeled intermediates was about the same (Figure 3b). On the contrary, complexes between the catalyst and solvent molecules ( $[(\text{PPh}_3)\text{Au}(\text{CH}_3\text{OH})]^+$  and  $[(\text{PPh}_3)\text{Au}(\text{CD}_3\text{OH})]^+$ ) are observed with a constant abundance ratio, because they are formed in a fast equilibrium that cannot be followed with the current technique.

The time evolution of the relative abundances of  $\text{E}^{\text{PPh}_3}$  and  $\text{D}_3\text{-E}^{\text{PPh}_3}$  can be seen in Figure 3c (note that the sum of  $\text{E}^{\text{PPh}_3}$  and  $\text{D}_3\text{-E}^{\text{PPh}_3}$  was normalized to 1. If we fit the relative abundances using eq 3a and 3b (the dashed lines in Figure 3), we obtain the rate constant  $k' \sim 0.063$  which corresponds to a half-life of  $\sim 11$  min (Table 3). We have examined the effect of the time delay (Table 2). The delay  $t_d$  should be sufficiently long so that an appreciable amount of the unlabeled product is formed. For very short time delays, the difference between the  $\text{E}^{\text{PPh}_3}$  and  $\text{D}_3\text{-E}^{\text{PPh}_3}$  relative abundances would be small and the determined half-life would be burdened by a large experimental error. The time delay should also not be too long, because then other effects come into play (e.g., degradation of catalyst, involvement of byproducts, etc.). If these principles are obeyed, then the effect of the time delay is rather small as evident from Table 2. We were able to obtain consistent results over large

**Table 2.** Effect of a Time Delay on the Determination of the Rate Constant  $k'$  for the Degradation of the Diaurated Intermediate  $\text{E}^{\text{PPh}_3}$  in the Reaction Catalyzed by  $[\text{AuCl}(\text{PPh}_3)]$  and the Rate Constant  $k$  for the Degradation of a Reactant Yielding the Diaurated Complex  $\text{E}^{\text{IPr}}$  in the Reaction Catalyzed by  $[\text{AuCl}(\text{IPr})]$

catalyst	time delay $t_d$ [min]	rate constant $k'$ [ $\text{min}^{-1}$ ]	half-life $t_{1/2}$	
2.5 mol % $[\text{AuCl}(\text{PPh}_3)]/ 3$ mol % $\text{AgSbF}_6$	2.5	$0.081 \pm 0.010$	$8.7 \pm 1.2$	
	10	$0.086 \pm 0.005$	$8.1 \pm 0.4$	
	30	$0.083 \pm 0.001$	$8.4 \pm 0.1$	
catalyst	time delay $t_d$ [min]	rate constant $k^{\text{MS}}$ [ $\text{min}^{-1}$ ]	$[\text{D}_3\text{-E}^{\text{IPr}}]_{\text{rel},\infty}$	$[\text{E}^{\text{IPr}}]_{\text{rel},t_d}$
2.5 mol % $[\text{AuCl}(\text{IPr})]/ 3$ mol % $\text{AgSbF}_6$	2.5	$0.13 \pm 0.06$	0.49	0.01
	5	$0.14 \pm 0.01$	0.46	0.08
	7.5	$0.13 \pm 0.02$	0.44	0.12
	10	$0.14 \pm 0.01$	0.40	0.20
	20	$0.10 \pm 0.02$	0.37	0.26

time delays. For the remaining experiments, we always took a time delay of 5 min.

We note in passing that for this series of experiments, a different batch of the gold catalyst was used and the rate constants were consistently by about 35% larger than in the remaining experiments listed in Table 3. We have also monitored the reaction by NMR using this new batch of the catalyst and it was by 37% faster (Figure S2a). We are showing these results to demonstrate that changes in reaction mixture are directly reflected by our experiments.

This approach gives us a powerful tool to study the effect of the reaction conditions on the half-life of the intermediates

**Table 3. Half-Lives Determined for the Diaurated Intermediates  $E^{\text{PPh}_3}$  in the Reaction Catalyzed by  $[\text{AuCl}(\text{PPh}_3)]$  and for the Diaurated Intermediates  $E^{\text{PMe}_3}$  and  $E^{\text{Mix}}$  in the Reaction Catalyzed by a Mixture of  $[\text{AuCl}(\text{PPh}_3)]$  and  $[\text{AuCl}(\text{IPr})]$** 

	catalyst	addition	additive	$E^{\text{PPh}_3} t_{1/2}$ [min]	rate constant $k'$ [ $\text{min}^{-1}$ ]
1	2.5 mol % $[\text{AuCl}(\text{PPh}_3)]/3$ mol % $\text{AgSbF}_6$	$\text{CD}_3\text{OH}$	–	$11.3 \pm 1.7$	$0.063 \pm 0.009$
2		$\text{CD}_3\text{OD}$	–	$12.2 \pm 0.8$	$0.057 \pm 0.004$
3		$\text{CD}_3\text{OH}$	TsOH	$7.0 \pm 1.6$	$0.101 \pm 0.023$
4		$\text{PhCCCH}_3, \text{CD}_3\text{OH}$	–	$7.3 \pm 0.6$	$0.096 \pm 0.009$
5		$\text{PhCCCH}_3, \text{CD}_3\text{OH}$	TsOH	$3.7 \pm 0.3$	$0.188 \pm 0.014$
6		$\text{PhCCCD}_3$	–	$4.2 \pm 0.4$	$0.167 \pm 0.018$
7	2.5 mol % $[\text{AuCl}(\text{PPh}_3)]/1.5$ mol % $\text{AgSbF}_6$	$\text{CD}_3\text{OH}$	–	$10.9 \pm 1.1$	$0.064 \pm 0.007$
8	2.5 mol % $[\text{AuCl}(\text{PPh}_3)]/6.0$ mol % $\text{AgSbF}_6$	$\text{CD}_3\text{OH}$	–	$10.3 \pm 0.8$	$0.068 \pm 0.005$
9	2.5 mol % $[\text{AuCl}(\text{PPh}_3)]/15$ mol % $\text{AgSbF}_6$	$\text{CD}_3\text{OH}$	–	$11.0 \pm 1.3$	$0.063 \pm 0.008$
				$E^{\text{PPh}_3} t_{1/2}$ [min]	$E^{\text{Mix}} t_{1/2}$ [min]
10	1.25 mol % $[\text{AuCl}(\text{PPh}_3)]/1.25$ mol % $[\text{AuCl}(\text{IPr})]/3$ mol % $\text{AgSbF}_6$	$\text{CD}_3\text{OD}$	–	$7.0 \pm 1.0$	$19.2 \pm 2.5$
11		$\text{CD}_3\text{OD}$	TsOH	$3.5 \pm 0.3$	$12.6 \pm 0.8$
12		$\text{CH}_3\text{OH}, \text{PhCCCD}_3$	–	$3.2 \pm 0.3$	$17.7 \pm 1.3$
13	2.5 mol % $[\text{AuCl}(\text{PPh}_3)]/1.25$ mol % $[\text{AuCl}(\text{IPr})]/4.5$ mol % $\text{AgSbF}_6$	$\text{CD}_3\text{OD}$	–	$8.1 \pm 1.4$	$16.2 \pm 1.9$
14	1.25 mol % $[\text{AuCl}(\text{PPh}_3)]/2.5$ mol % $[\text{AuCl}(\text{IPr})]/4.5$ mol % $\text{AgSbF}_6$	$\text{CD}_3\text{OD}$	–	not detected	$19.9 \pm 4.5$
15	2.5 mol % $[\text{AuCl}(\text{PPh}_3)]/2.5$ mol % $[\text{AuCl}(\text{IPr})]/6$ mol % $\text{AgSbF}_6$	$\text{CD}_3\text{OD}$	–	$8.4 \pm 2.4$	$14.5 \pm 1.5$
				$E^{\text{PMe}_3} t_{1/2}$ [min]	rate constant $k'$ [ $\text{min}^{-1}$ ]
16	2.5 mol % $[\text{AuCl}(\text{PMe}_3)]/3$ mol % $\text{AgSbF}_6^a$	$\text{CD}_3\text{OD}$		$4.0 \pm 0.3^a$	$0.17 \pm 0.1^a$

<sup>a</sup>Values are derived from previously published kinetics for the  $[(\text{PMe}_3)_2\text{Au}_2(\text{PhCCMe}, \text{OCH}_3)]^+$  intermediate detected for the reaction performed under the same condition with the  $[\text{AuCl}(\text{PMe}_3)]$  catalyst.<sup>13</sup>

(average of several measurements for each experiment together with the derived experimental error can be found in Table 3). First, we have tested whether the labeling of the reaction mixture with  $\text{CD}_3\text{OD}$  instead of  $\text{CD}_3\text{OH}$  would result in significant changes (Entries 1 and 2 in Table 3). The derived half-lives are slightly longer than those obtained with  $\text{CD}_3\text{OH}$ , but the effect is in the range of the experimental error (more results with  $\text{CD}_3\text{OD}$  can be found in the Supporting Information). Second, we have investigated the effect of acid addition (Entry 3). Addition of 4 mol % of *p*-toluenesulfonic acid (TsOH) results in a decrease of the half-life of the  $[(\text{PPh}_3)_2\text{Au}_2(\text{PhCCMe}, \text{OCH}_3)]^+$  intermediate to 7 min, hence almost to one-half (experimental data are shown in gray in Figure 3c). This is consistent with a view that the acid catalyzed protodeauration step is responsible for the depletion of the diaurated intermediates.

We have also tested the effect of silver salt addition on the half-life of the diaurated intermediates (Entries 7–9). In some of the gold-catalyzed reactions, a peculiar silver effect was observed that accelerated or even enabled the given reactions.<sup>41</sup> We have measured the diaurated intermediate half-lives in dependence of the silver cations' concentration. The results show that for the ratios of  $[\text{AuCl}(\text{PPh}_3)]$  to  $[\text{AgSbF}_6]$  ranging from 1:0.5 via 1:1.2 to 1:5 the half-lives of the diaurated intermediates are the same within the experimental error. It means that we do not observe any participation of the silver cations in the depletion of the diaurated intermediates. We note in passing that we have performed NMR experiments with a large excess of the silver salt concentration and in agreement, no effect on the overall reactivity was found (Figure S2b in the Supporting Information).<sup>42,43</sup>

It is interesting to note that the half-life of the diaurated intermediates did not change even when the concentration of the silver salt was only half of that of the gold catalyst (Entry 7). Probably, a lower concentration of the active catalyst in the reaction mixture was investigated in this experiment, but it did not influence the determined half-life of the diaurated intermediates.

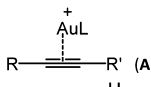
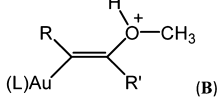
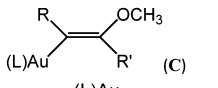
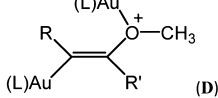
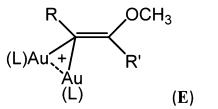
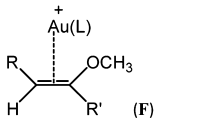
Besides reaction-mixture labeling with  $\text{CD}_3\text{OH}$ , we can label other reactants, e.g., 1-phenylpropyne as was previously mentioned. Using  $\text{Ph}-\text{CC}-\text{CD}_3$  we have obtained a half-life for the  $E^{\text{PPh}_3}$  diaurated intermediates of 4.2 min (Entry 6). As we have added only an equimolar amount of  $\text{Ph}-\text{CC}-\text{CD}_3$  to the standard reaction solution, we were working with a 2-fold catalyst and 4-fold alkyne concentrations in the final reaction mixture. In order to keep the concentration equal in the remaining experiments and just double the concentration of the alkyne, we have labeled the reaction mixture with  $\text{CD}_3\text{OH}$  and one additional equivalent of  $\text{Ph}-\text{CC}-\text{CH}_3$  (Entry 4). This experiment gives a half-life for the diaurated intermediates of 7.3 min. It clearly shows that the alkyne plays a role in the decomposition of the diaurated intermediates. Finally, we have repeated the same experiment with  $\text{CD}_3\text{OH}/\text{Ph}-\text{CC}-\text{CH}_3$  labeling, but with addition of 4 mol % of *p*-toluenesulfonic acid (Entry 5). As expected, it resulted in a further decrease of the half-life. Consistently with the results above, the half-life dropped to about one-half (3.7 min).

We have also performed the same experiments with the  $[\text{AuCl}(\text{IPr})]$  catalyst (Figure 3d). Already at first sight, it is clear that the shapes of the curves representing the relative abundances of the unlabeled and labeled signals do not correspond to the establishment of steady-state conditions. If we assume that the  $E^{\text{IPr}}$  diaurated complexes do not decompose at all as suggested earlier<sup>27</sup> and that the unlabeled  $E^{\text{IPr}}$  and labeled  $\text{D}_3\text{-E}^{\text{IPr}}$  complexes are formed with the same rate, then we can fit the curve for the labeled product with a simple exponential function:

$$[\text{Prod}^{\text{label}}]_{\text{rel},t} = [\text{Prod}^{\text{label}}]_{\text{rel},\infty} - \alpha e^{-k^{\text{MS}}(t+t_1)} \quad (4)$$

This expression assumes normalization of  $[\text{Prod}] + [\text{Prod}^{\text{label}}] = 1$ . At the end of the reaction, we obtain the relative yields of the labeled product  $[\text{Prod}^{\text{label}}]_{\text{rel},\infty}$  and that of the unlabeled product  $[\text{Prod}]_{\text{rel},\infty} = 1 - [\text{Prod}^{\text{label}}]_{\text{rel},\infty}$  in that  $[\text{Prod}]_{\text{rel},t_1} = (1 - 2[\text{Prod}^{\text{label}}]_{\text{rel},\infty})$  was formed during the delay before the labeling of the reaction mixture. The exponential

**Table 4. Relative Energies ( $\Delta\Delta H^{298\text{ K}}_{\text{MeOH}}$  and  $\Delta\Delta H^{298\text{ K}}_{\text{GP}}$ )<sup>a</sup> in  $\text{kJ mol}^{-1}$  of Different Intermediates on the B3LYP-D3/cc-pVTZ:LanL2DZ(Au) Potential Energy Surface for the Gold Mediated Methanol Addition to 1-Phenylpropyne**

Intermediates	Reactants/ Catalysts/ Products	C(1) addition	C(2) addition	C(1) addition	C(2) addition
		L = PPh <sub>3</sub>	L = PPh <sub>3</sub>	L = IPr	L = IPr
		$\Delta\Delta H^{298\text{ K}}_{\text{MeOH}}$ [kJ mol <sup>-1</sup> ] ( $\Delta\Delta H^{298\text{ K}}_{\text{GP}}$ [kJ mol <sup>-1</sup> ])			
	3x 1-phenylpropyne 2x [(L)Au(CH <sub>3</sub> OH)] <sup>+</sup> 2x CH <sub>3</sub> OH	0 (0)	0 (0)	0 (0)	0 (0)
 (A)	2x 1-phenylpropyne [(L)Au(CH <sub>3</sub> OH)] <sup>+</sup> 3x CH <sub>3</sub> OH	-14 (-31)	-14 (-31)	-32 (-48)	-32 (-48)
 (B)	2x 1-phenylpropyne [(L)Au(CH <sub>3</sub> OH)] <sup>+</sup> 2x CH <sub>3</sub> OH	25 <sup>b</sup>	<i>16<sup>b</sup>, 18 (-8)</i>	not found	11 (-13)
 (C)	2x 1-phenylpropyne [(L)Au(CH <sub>3</sub> OH)] <sup>+</sup> (CH <sub>3</sub> OH) <sub>2</sub> H <sup>+</sup>	-31 <sup>c</sup> (24) <sup>c</sup> -23 <sup>d</sup> (38) <sup>d</sup>	-31 (33)	-30 (40)	-34 (38)
 (D)	2x 1-phenylpropyne CH <sub>3</sub> OH (CH <sub>3</sub> OH) <sub>2</sub> H <sup>+</sup>	-68 (-56)	-82 (-70)	-83 (-64)	-88 (-64)
 (E)	2x 1-phenylpropyne CH <sub>3</sub> OH (CH <sub>3</sub> OH) <sub>2</sub> H <sup>+</sup>	-149 (-141)	-153 (-140)	-137 (-124)	-155 (-135)
 (F)	2x 1-phenylpropyne [(L)Au(CH <sub>3</sub> OH)] <sup>+</sup> 2x CH <sub>3</sub> OH	-126 (-157)	-141 (-165)	-141 (-172)	-157 (-181)
F + A	1-phenylpropyne 3x CH <sub>3</sub> OH	-140 (-188)	-155 (-197)	-173 (-220)	-189 (-229)
	Product 2x 1-phenylpropyne 2x [(L)Au(CH <sub>3</sub> OH)] <sup>+</sup> CH <sub>3</sub> OH	-97 (-110)	-106 (-114)	-97 (-110)	-106 (-114)
A	Product 1-phenylpropyne [(L)Au(CH <sub>3</sub> OH)] <sup>+</sup> 2x CH <sub>3</sub> OH	-111 (-141)	-121 (-145)	-129 (-158)	-138 (-162)
2x A	Product 3x CH <sub>3</sub> OH	-126 (-172)	-135 (-177)	-161 (-206)	-170 (-210)

<sup>a</sup>The geometries were optimized in the gas phase, and the solvation energies in methanol were calculated using PCM method. <sup>b</sup>Geometries of the B intermediates were optimized using the PCM solvation model (values are given in italics). The B adducts corresponding to C(1) addition do not represent minima on the potential energy surface in vacuum. <sup>c</sup>Small imaginary frequency resulted always from the calculations for this stationary point. We have applied a thermal correction to enthalpy from the other conformer of this isomer. <sup>d</sup>A second possible conformer of the C(1) monoaurated intermediate. It is slightly higher in energy; all second derivatives were positive.

function expresses the decay of the reactant from which the diaurated complex is formed multiplied by the fitting parameter  $\alpha$ .

The solid lines in Figure 3d show fits of the results obtained with different time-delays and Table 2 lists the fitted parameters. The model correctly shows that with the prolongation of the time-delay  $t_d$  the relative yield of the unlabeled product  $[E^{\text{IPr}}]_{\text{rel},t_d}$  formed during this time grows. The rate constant determined for the degradation of the reactant that provides the diaurated complexes (i.e., most probably 1-phenylpropyne) under the conditions of the experiment is estimated as  $0.13 \pm 0.02 \text{ min}^{-1}$  (average of the  $k^{\text{MS}}$  values listed in Table 2). For comparison, the value obtained from the kinetic modeling of the NMR results is  $0.135 \text{ min}^{-1}$  (i.e.,  $(k_1^{\text{NMR}} + k_2^{\text{NMR}}) \cdot [\text{Au}(\text{IPr})]^+ = 22.5 \cdot 0.006$ ), which is in very good agreement. As the determination of the kinetics for the reactants and products is not the aim of this paper, we do not elaborate it further.

The last experiment involves the determination of the half-times of the intermediates in the reaction catalyzed by a mixture of the  $[\text{AuCl}(\text{PPh}_3)]$  and  $[\text{AuCl}(\text{IPr})]$  catalysts. We can observe not only the homodiaurated intermediates  $[(\text{PPh}_3)_2\text{Au}_2(\text{PhCCMe}, \text{OCH}_3)]^+$  and  $[(\text{IPr})_2\text{Au}_2(\text{PhCCMe}, \text{OCH}_3)]^+$ , but also—the overwhelmingly dominant signal in the ESI-MS spectrum of this reaction mixture—the mixed  $[(\text{PPh}_3)(\text{IPr})\text{Au}_2(\text{PhCCMe}, \text{OCH}_3)]^+$  intermediate. The diaurated intermediate with two carbene ligands  $[(\text{IPr})_2\text{Au}_2(\text{PhCCMe}, \text{OCH}_3)]^+$  was very low abundant; in some of the experiments it was not even detected (see the Supporting Information).

The rate constant determined for the degradation of  $[(\text{PPh}_3)_2\text{Au}_2(\text{PhCCMe}, \text{OCH}_3)]^+$  in the reaction mixture with both catalysts is larger than that determined in the reaction mixture with the (triphenylphosphino)gold catalyst only. Using delayed labeling by CD<sub>3</sub>OD, the half-times of the intermediates drop to about one-half both without and with the addition of the TsOH acid (7.0 and 3.5 min, respectively; Entries 10 and

11 in Table 3). The half-lives of the mixed  $[(\text{PPh}_3)(\text{IPr})\text{Au}_2(\text{PhCCMe}, \text{OCH}_3)]^+$  ( $\text{E}^{\text{Mix}}$ ) intermediates are considerably longer. It is important to note that during the equilibration of the concentrations of the  $\text{E}^{\text{Mix}}$  and  $\text{D}_3\text{-E}^{\text{Mix}}$  intermediates, the alkyne reactant is largely depleted (compare with the NMR experiments). It will surely lead to a decreasing rate of intermediate formation which can lead to the decreasing of their signal intensities in the MS spectrum. Nevertheless, the rate constant  $k'$  determined according to eq 3a should not be significantly influenced. The  $\text{E}^{\text{Mix}}$  half-life in the reaction mixture is about 19 min and with the addition of 4 mol % of TsOH it drops to about 13 min. Labeling of the reaction mixture with the Ph-CC-CD<sub>3</sub> reactant leads again to a faster degradation of the diaurated intermediates with the half-life of  $[(\text{PPh}_3)_2\text{Au}_2(\text{PhCCMe}, \text{OCH}_3)]^+$  determined as 3.2 min and that of  $[(\text{PPh}_3)(\text{IPr})\text{Au}_2(\text{PhCCMe}, \text{OCH}_3)]^+$  as 17.7 min (Entry 12). We have performed the same experiments with different concentrations and proportions of the catalysts and we have not determined any significant influence on the determined half-lives (Entries 13–15).

**DFT Calculations.** In order to aid the discussion of the results, we have performed exploratory DFT calculations with an implicit methanol solvation model (Table 4). The relative energies are given with respect to the separated reactant molecules (1-phenylpropyne and methanol) and the methanol adduct of the catalyst (i.e.,  $[(\text{L})\text{Au}(\text{CH}_3\text{OH})]^+$ , where  $\text{L} = \text{PPh}_3$  or IPr). For the deprotonation steps, we have assumed the formation of proton-bound methanol dimer (see the Computational Details). The energies in Table 4 are calculated on one potential energy surface and the molecules/ions considered for each minimum are listed in the first two columns.

The initial formation of the complex between the catalyst and 1-phenylpropyne is exothermic by 14 kJ mol<sup>-1</sup> for  $\text{L} = \text{PPh}_3$  and 32 kJ mol<sup>-1</sup>  $\text{L} = \text{IPr}$ . The addition of a methanol molecule to these complexes is endothermic by 32 and 43 kJ mol<sup>-1</sup>, respectively. We have located this high-energy intermediate only for the methanol addition to the C(2) position of 1-phenylpropyne. All attempts to localize the C(1) methanol adduct in the gas phase resulted in its dissociation back to the reactants. It was possible to find these intermediates if we performed the geometry optimization with the methanol solvation effect. These values are given in italics in Table 4.

The next step has to be associated with deprotonation. Simple deprotonation is exothermic by about 50 kJ mol<sup>-1</sup>. Formation of the C(2) addition product is slightly more preferred, but the differences are only on the order of units of kJ mol<sup>-1</sup>. Exchange of the proton by the  $[(\text{L})\text{Au}]^+$  cation at the oxygen atom is exothermic by almost 100 kJ mol<sup>-1</sup> and again formation of the C(2) product is preferred. The alternative deprotonation associated with the direct formation of the geminally diaurated intermediate is the most exothermic process with an energy gain of more than 150 kJ mol<sup>-1</sup>. Regioselectivity is again slightly in favor of the formation of the C(2) product.

The monoaurated intermediate can be protonated, which directly leads to the gold complex of the product ( $\text{C} + \text{H}^+ \rightarrow \text{F}$ ). This process is exothermic by more than 100 kJ mol<sup>-1</sup> and should thus be facile. Alternatively, the protonation can be associated with deauration, but it is by about 40 kJ mol<sup>-1</sup> ( $\text{L} = \text{PPh}_3$ ) or 50 kJ mol<sup>-1</sup> ( $\text{L} = \text{IPr}$ ) less energy favored. The diaurated intermediates can decompose by protodeauration leading to the gold complex of the product (F). This step is endothermic by about 10–15 kJ mol<sup>-1</sup> for  $\text{L} = \text{PPh}_3$  and almost

thermoneutral for  $\text{L} = \text{IPr}$ . If we consider protodeauration associated with the transfer of one of the gold cations to the alkyne reactant (as suggested by the experimental results), the process becomes thermoneutral for  $\text{L} = \text{PPh}_3$  and exothermic for  $\text{L} = \text{IPr}$ .

The computational results do not give any significant lead as to why the regioselectivity of the first addition of methanol to 1-phenylpropyne differs on changing the ancillary ligand at the gold catalyst. It also does not show why the reaction with  $[(\text{PPh}_3)\text{Au}]^+$  leads to the diaurated intermediates opposed to the reactions with  $[(\text{IPr})\text{Au}]^+$ . The energy profiles for both reactions are rather similar. Note that solvation is considered by an implicit model. Using this approach, it is not possible to unravel solvation steric effects that play very significant role in this reaction as is discussed below.

## DISCUSSION

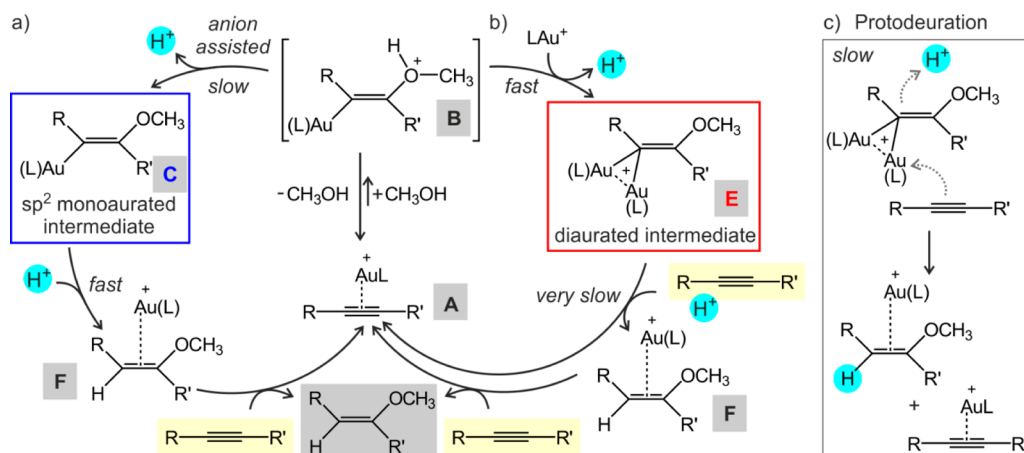
The NMR data for the “ $[(\text{IPr})\text{Au}]^+$ ” catalyzed reaction shows that the first methanol addition is several times faster than the second one and the methoxy group addition proceeds preferentially to the C(2) position of 1-phenylpropyne. Both reaction steps are accelerated by acid addition with acceleration of the second methanol addition more pronounced. The acceleration caused by acid addition (i.e., TsOH here) can either suggest that the protodeauration step is the rate-determining step,<sup>44</sup> or that there is active involvement of the anions in the initial deprotonation of adduct B to form neutral monoaurated intermediates.<sup>45</sup> Tosylate was suggested as particularly favorable anion.<sup>46–48</sup> The ESI-MS delayed reactant labeling method shows that the diaurated complexes  $[(\text{IPr})_2\text{Au}_2(\text{PhCCMe}, \text{OCH}_3)]^+$  are not in equilibrium with either the reactants or products, but rather formed as stable complexes, i.e., byproducts. The reaction therefore does not proceed via their formation.

The reaction catalyzed by “ $[(\text{PPh}_3)\text{Au}]^+$ ” is slower than the “ $[(\text{IPr})\text{Au}]^+$ ” catalyzed one due to the considerable deceleration of the first methanol addition to the alkyne. The second methanol addition is an order of magnitude faster than the first one and it is also faster than the analogous reaction catalyzed by “ $[(\text{IPr})\text{Au}]^+$ ”. The regioselectivity is switched toward the preferential methoxy addition to the C(1) position of 1-phenylpropyne. Both reaction steps are again accelerated by the acid addition. The most obvious explanation of the deterioration of the “ $[(\text{PPh}_3)\text{Au}]^+$ ” mediated reaction lies in the formation of the diaurated intermediates.

The delayed reactant labeling ESI-MS experiments show that the  $[(\text{PPh}_3)_2\text{Au}_2(\text{PhCCMe}, \text{OCH}_3)]^+$  formation and depletion can be approximated by steady-state conditions. The determined rate constants are associated with the depletion of the  $\text{E}^{\text{PPh}_3}$  intermediates. It clearly shows that the addition of 4 mol % of TsOH increases the depletion rate constant by about 50%. In comparison, the NMR experiments show that the reaction rates for the first methanol addition to the C(1) and C(2) position increase on acid addition by 37% and 50%, respectively. This nice agreement suggests that depletion of the diaurated intermediates is the rate-determining step in this reaction. Second, we have shown that doubling the concentration of the alkyne also leads to an increase of the rate constant for the depletion of the diaurated intermediates. It means that the alkyne takes an active part in the process, which might thus correspond to transmetalation.

Next to the effect of the acid, which is exposed in the same way to the rate of the diaurated intermediate depletion as the



Scheme 3. Suggested Reaction Mechanism<sup>a</sup>

<sup>a</sup>(a) Mechanism for the reactions catalyzed by  $[\text{Au}(\text{L})]^+$ , where L is bulky. (b) Dual activation mechanism catalyzed by  $[\text{Au}(\text{L})]^+$  for which the  $[\text{Au}(\text{L})]^+ \rightleftharpoons \text{H}^+$  exchange is faster than unassisted deprotonation. (c) Protodeauration of diaurated intermediates assisted by the alkyne reactant.

overall reaction rate, it is interesting to note similar relationships between the  $[(\text{PPh}_3)\text{Au}]^+$  catalyzed reaction and the previously published reaction catalyzed by  $[(\text{PMe}_3)\text{Au}]^+$ . The slower rate of  $[(\text{PPh}_3)_2\text{Au}_2(\text{PhCCMe},\text{OCH}_3)]^+$  decomposition ( $k'_{\text{PPh}_3}:k'_{\text{PMe}_3} = 0.06:0.17$ , see Table 3) translates quite well to the slower reaction rate of 1-phenylpropyne with methanol determined by the NMR experiments. This is strong support for the reaction pathway taking place via the diaurated intermediates. An alternative explanation involves a side equilibrium between the monoaurated and diaurated intermediates. If it would hold true, we would expect formation as well as decomposition of  $[(\text{PPh}_3)_2\text{Au}_2(\text{PhCCMe},\text{OCH}_3)]^+$  at a slower rate than the formation and decomposition of  $[(\text{PMe}_3)_2\text{Au}_2(\text{PhCCMe},\text{OCH}_3)]^+$  due to steric effects. The slower formation of the  $[(\text{PPh}_3)_2\text{Au}_2(\text{PhCCMe},\text{OCH}_3)]^+$  intermediates would result in a faster reaction cycling via the monoaurated intermediates. Hence, the overall reaction would be expected to be faster than the reaction catalyzed by  $[(\text{PMe}_3)\text{Au}]^+$ . Such a scenario is observed for the  $[(\text{IPr})\text{Au}]^+$  catalyzed reaction, but not for that catalyzed by  $[(\text{PPh}_3)\text{Au}]^+$ .

The experiment with the mixture of  $[(\text{PPh}_3)\text{Au}]^+$  and  $[(\text{IPr})\text{Au}]^+$  catalysts shows that the first methanol addition is mainly mediated by  $[(\text{IPr})\text{Au}]^+$  as it is faster than in the reaction with  $[(\text{PPh}_3)\text{Au}]^+$  alone and it has the same selectivity toward the C(2) addition as the reaction solely with  $[(\text{IPr})\text{Au}]^+$ . The second methanol addition is mediated by  $[(\text{PPh}_3)\text{Au}]^+$  as the reaction rates are almost the same. The first reaction step is slowed down about seven times in comparison with the  $[(\text{IPr})\text{Au}]^+$  catalyzed reaction. Clearly the reason is the formation of the mixed diaurated intermediates  $[(\text{PPh}_3)(\text{IPr})\text{Au}_2(\text{PhCCMe},\text{OCH}_3)]^+$  ( $\text{E}^{\text{Mix}}$ ) which fully decompose but at a very slow rate.

What is the origin of these mixed diaurated intermediates? The formation of these intermediates is not sterically hindered as it was the case for those bearing two IPr ligands ( $[(\text{IPr})_2\text{Au}_2(\text{PhCCMe},\text{OCH}_3)]^+$ ). From the drop of the rate we know that about 2/3 of the  $[(\text{IPr})\text{Au}]^+$  cations are blocked in the diaurated intermediates. It also suggests that most of the  $[(\text{PPh}_3)\text{Au}]^+$  cations are blocked in the  $\text{E}^{\text{Mix}}$  intermediates. The prevalence of the mixed intermediates is associated with their stability which leads to their accumulation with time. The

shorter half-life of the  $\text{E}^{\text{PPh}_3}$  intermediates in the reaction mixture containing  $[(\text{IPr})\text{Au}]^+$  cations is probably associated with the faster formation of the vinylother primary products that can take part in transmetalation of the diaurated intermediates similar to what was observed for the alkyne reactant. The interaction energy of  $[(\text{PPh}_3)\text{Au}]^+$  with the vinylother products amounts to  $29 \text{ kJ mol}^{-1}$  for the C(1) product and  $35 \text{ kJ mol}^{-1}$  for the C(2) product, hence larger than with the alkyne ( $14 \text{ kJ mol}^{-1}$ ).

On the basis of all of the experimental data and computational results, we suggest the following reaction mechanism (Scheme 3). The initial addition of the methanol molecule to the gold-activated alkyne is a reversible endothermic step. The selectivity toward C(1) or C(2) addition is given by the following irreversible step. It can be a simple deprotonation and then the selectivity will be tuned toward the formation of the more stable monoaurated intermediate. In addition, steric effects can also play a role: In the C(1) addition product, the ligated gold cation is bound to the C(2) carbon with a Z-configuration relative to the reactant phenyl ring. This might represent a steric hindrance for the formation of the C(1) addition product. The deprotonation can be catalyzed by the anions in the reaction mixture.

The alternative deprotonation pathway is assisted by the intake of another  $[(\text{L})\text{Au}]^+$  cation. This reaction is strongly exothermic and is most probably kinetically controlled. The initial B adduct corresponding to the C(2) addition has the phenyl group in the geminal position with the  $[(\text{L})\text{Au}]^+$  unit (Figure 4). The phenyl group is turned out of the plane and sterically shades the carbon to be attacked by the second  $[(\text{L})\text{Au}]^+$  cation. The intermediate with the methanol molecule attached to the C(1) carbon atom is less sterically hindered for the attack of the second  $[(\text{L})\text{Au}]^+$  cation. Note that for the small  $[(\text{PMe}_3)\text{Au}]^+$  catalyst, where steric effects play a less important role, the thermodynamically preferred C(2) product is formed. The gold-assisted deprotonation is probably much faster than the unassisted or anion-assisted deprotonation and that is why the reaction pathway leads via the formation of the diaurated intermediates. It can only be suppressed, if the  $[(\text{L})\text{Au}]^+$  cations bear sufficiently bulky ancillary ligands L (i.e., IPr here).

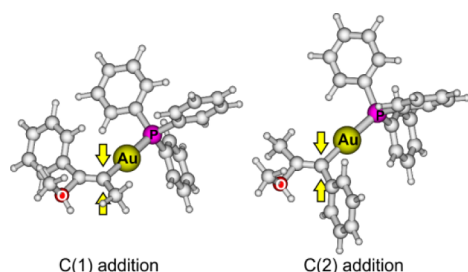


**Figure 4.** Suggested reaction coordinates for the gold assisted deprotonation of the methanol adduct. The yellow arrows show the carbon atom attacked by the second gold cation. The attacks would be probably favorable from the bottom of the complexes. The C(2) intermediate is more sterically hindered due to the phenyl group. The structures were obtained by the geometry optimization (B3LYP-D3/cc-pVTZ:LanL2DZ(Au)) in methanol using the PCM model.

As shown by our delayed reactant labeling experiments, the degradation of the diaurated intermediates is first-order dependent on the alkyne concentration and it is catalyzed by acid. We suggest that the protodeauration proceeds to form the gold-complex of the alkyne and the gold complex of the product (see Scheme 3c). Clearly, protonation of the neutral monoaurated intermediate will be much faster than that of the positively charged diaurated intermediate. This explains why the reaction catalyzed by a bulky catalyst, which blocks the reaction pathway via the diaurated intermediates, is faster than that catalyzed by a sterically less demanding catalyst. For the second methanol addition, no diaurated intermediates can be formed. The reaction is therefore faster with the less bulky catalyst, because the formation of the monoaurated intermediate as well as the protodeauration reaction are less sterically hindered.

## CONCLUSIONS

We present a new method for extraction of kinetic data for intermediates in reaction mixtures under the condition that they are observable by ESI-MS. We have demonstrated that for intermediates formed in a steady-state approximation, the effect of reaction conditions on their half-life can be extracted. The effect of, e.g., acidity, catalyst concentration, or substrate concentration can be studied. In connection to the classical kinetics obtained from NMR experiments, this method can bring unprecedented data on key low-abundant intermediates.

The method was applied for the investigation of diaurated intermediates in methanol addition to alkynes. The diaurated complexes were considered to be off-cycle intermediates that slow down the addition reaction because of the catalyst being retained as diaurated complexes. We have shown here that they are not off-cycle intermediates. The initial gold-mediated methanol addition is an endothermic step. The driving force toward the products is the exchange of the proton bound to the oxygen atom by a gold cation, leading to the diaurated intermediates. Their protodeauration is a slow process and therefore the overall reaction is slow. This reaction pathway can be suppressed, if the gold cations bear sterically demanding ancillary ligands such as a *N*-heterocyclic carbene ligand IPr. The reaction then dominantly proceeds by the simple deprotonation step toward monoaurated intermediates. While the initial deprotonation step is slow, the overall reaction is faster, because protodeauration of the monoaurated intermediates is easier than with the diaurated intermediates.

## ASSOCIATED CONTENT

### Supporting Information

The Supporting Information is available free of charge on the ACS Publications website at DOI: 10.1021/jacs.5b08744.

Further experimental details, NMR spectra, ESI-MS spectra, delayed reactant labeling experiments, further computational results, and geometries of all optimized structures. (PDF)

## AUTHOR INFORMATION

### Corresponding Author

\*roithova@natur.cuni.cz

### Notes

The authors declare no competing financial interest.

## ACKNOWLEDGMENTS

This work was supported by the Grant Agency of the Czech Republic (14-20077S) and the European Research Council (StG ISORI). The authors thank Dr. Andrew Gray for his help in preparing the manuscript.

## REFERENCES

- Chen, P. *Angew. Chem., Int. Ed.* **2003**, *42*, 2832.
- Yunker, L. P. E.; Stoddard, R. L.; McIndoe, J. S. *J. Mass Spectrom.* **2014**, *49*, 1.
- O'Hair, R. A. J. *Int. J. Mass Spectrom.* **2015**, *377*, 121.
- Schröder, D. *Acc. Chem. Res.* **2012**, *45*, 1521.
- Vikse, K. L.; Ahmadi, Z.; McIndoe, J. S. *Coord. Chem. Rev.* **2014**, *279*, 96.
- Eberlin, M. N. *Eur. Mass Spectrom.* **2007**, *13*, 19.
- Bock, K.; Feil, J. E.; Karaghiosoff, K.; Koszinowski, K. *Chem. - Eur. J.* **2015**, *21*, 5548.
- Kretschmer, R.; Schlangen, M.; Schwarz, H. *Chem. - Eur. J.* **2012**, *18*, 40.
- Santos, L. S. *Eur. J. Org. Chem.* **2008**, *2008*, 235.
- Ringger, D. H.; Kobylanski, I. J.; Serra, D.; Chen, P. *Chem. - Eur. J.* **2014**, *20*, 14270.
- Roithová, J. *Chem. Soc. Rev.* **2012**, *41*, 547.
- Oomens, J.; Sartakov, B. G.; Meijer, G.; Von Helden, G. *Int. J. Mass Spectrom.* **2006**, *254*, 1.
- Roithova, J.; Jankova, S.; Jasikova, L.; Vana, J.; Hybelbauerova, S. *Angew. Chem., Int. Ed.* **2012**, *51*, 8378.
- Kohler, M.; Leary, J. A. *Int. J. Mass Spectrom. Ion Processes* **1997**, *162*, 17.
- Schröder, D.; Weiske, T.; Schwarz, H. *Int. J. Mass Spectrom.* **2002**, *219*, 729.
- Schröder, D. *Phys. Chem. Chem. Phys.* **2012**, *14*, 6382.
- Vikse, K. L.; Ahmadi, Z.; Manning, C. C.; Harrington, D. A.; McIndoe, J. S. *Angew. Chem., Int. Ed.* **2011**, *50*, 8304.
- Limberger, J.; Leal, B. C.; Monteiro, A. L.; Dupont, J. *Chem. Sci.* **2015**, *6*, 77.
- von Rekowski, F.; Koch, C.; Gschwind, R. M. *J. Am. Chem. Soc.* **2014**, *136*, 11389.
- For the review on diaurated intermediates, see: Hashmi, A. S. K. *Acc. Chem. Res.* **2014**, *47*, 864.
- Lein, M.; Rudolph, M.; Hashmi, A. S. K.; Schwerdtfeger, P. *Organometallics* **2010**, *29*, 2206.
- Mizushima, E.; Sato, K.; Hayashi, T.; Tanaka, M. *Angew. Chem., Int. Ed.* **2002**, *41*, 4563.
- Kovács, G.; Ujaque, G.; Lledós, A. *J. Am. Chem. Soc.* **2008**, *130*, 853.
- Nolan, S. P. *Acc. Chem. Res.* **2011**, *44*, 91.
- Obradors, C.; Echavarren, A. M. *Chem. Commun.* **2014**, *50*, 16.
- Roithova, J.; Hrusak, J.; Schröder, D.; Schwarz, H. *Inorg. Chim. Acta* **2005**, *358*, 4287.

- (27) Zhdanko, A.; Maier, M. E. *Chem. - Eur. J.* **2014**, *20*, 1918.
- (28) Hashmi, A. S. K.; Schuster, A. M.; Rominger, F. *Angew. Chem., Int. Ed.* **2009**, *48*, 8247.
- (29) Liu, L. R.; Hammond, G. B. *Chem. Soc. Rev.* **2012**, *41*, 3129.
- (30) Seidel, G.; Lehmann, C. W.; Fürstner, A. *Angew. Chem., Int. Ed.* **2010**, *49*, 8466.
- (31) Weber, D.; Tarselli, M. A.; Gagne, M. R. *Angew. Chem., Int. Ed.* **2009**, *48*, 5733.
- (32) Simonneau, A.; Jaroschik, F.; Lesage, D.; Karanik, M.; Guillot, R.; Malacria, M.; Tabet, J. C.; Goddard, J. P.; Fensterbank, L.; Gandon, V.; Gimbert, Y. *Chem. Sci.* **2011**, *2*, 2417.
- (33) Weber, D.; Jones, T. D.; Adduci, L. L.; Gagne, M. R. *Angew. Chem., Int. Ed.* **2012**, *51*, 2452.
- (34) Ducháčková, L.; Roithová, J. *Chem. - Eur. J.* **2009**, *15*, 13399.
- (35) Jašíková, L.; Roithová, J. *Organometallics* **2012**, *31*, 1935.
- (36) (a) Vosko, S. H.; Wilk, L.; Nusair, M. *Can. J. Phys.* **1980**, *58*, 1200. (b) Lee, C.; Yang, W.; Parr, R. G. *Phys. Rev. B: Condens. Matter Mater. Phys.* **1988**, *37*, 785. (c) Becke, A. D. *J. Chem. Phys.* **1993**, *98*, 5648. (d) Stephens, P. J.; Devlin, F. J.; Chabalowski, C. F.; Frisch, M. J. *J. Phys. Chem.* **1994**, *98*, 11623.
- (37) Grimme, S.; Antony, J.; Ehrlich, S.; Krieg, H. *J. Chem. Phys.* **2010**, *132*, 154104.
- (38) Frisch, M. J. et al. *Gaussian 09*, Revision A.02; Gaussian, Inc.: Wallingford, CT, 2009.
- (39) Tomasi, J.; Mennucci, B.; Cammi, R. *Chem. Rev.* **2005**, *105*, 2999.
- (40) Fifen, J. J.; Nsangou, M.; Dhaouadi, Z.; Motapon, O.; Jaidane, N. E. *J. Chem. Theory Comput.* **2013**, *9*, 1173.
- (41) Wang, D.; Cai, R.; Sharma, S.; Jirak, J.; Thummanapelli, S. K.; Akhmedov, N. G.; Zhang, H.; Liu, X.; Petersen, J. L.; Shi, X. *J. Am. Chem. Soc.* **2012**, *134*, 9012.
- (42) Ranieri, B.; Escofet, I.; Echavarren, A. M. *Org. Biomol. Chem.* **2015**, *13*, 7103.
- (43) Zhdanko, A.; Maier, M. E. *ACS Catal.* **2015**, *5*, 5994.
- (44) Brown, T. J.; Weber, D.; Gagne, M. R.; Widenhofer, R. A. *J. Am. Chem. Soc.* **2012**, *134*, 9134.
- (45) Jia, M.; Bandini, M. *ACS Catal.* **2015**, *5*, 1638.
- (46) Biasiolo, L.; Trinchillo, M.; Belanzoni, P.; Belpassi, L.; Busico, V.; Ciancaleoni, G.; D'Amora, A.; Macchioni, A.; Tarantelli, F.; Zuccaccia, D. *Chem. - Eur. J.* **2014**, *20*, 14594.
- (47) Biasiolo, L.; Del Zotto, A.; Zuccaccia, D. *Organometallics* **2015**, *34*, 1759.
- (48) Ciancaleoni, G.; Belpassi, L.; Zuccaccia, D.; Tarantelli, F.; Belanzoni, P. *ACS Catal.* **2015**, *5*, 803.